Photoluminescence of Anatase and Rutile TiO_2 Particles†

Nadica D. Abazović,‡ Mirjana I. Čomor,‡ Miroslav D. Dramićanin,‡ Dragana J. Jovanović,‡ S. Phillip Ahrenkiel,§ and Jovan M. Nedeljković*,‡

Vinča Institute of Nuclear Sciences, P.O. Box 522, 11001 Belgrade, Serbia, and National Renewable Energy Laboratory, 1617 Cole Boulevard, Golden, Colorado 80401

Received: July 14, 2006; In Final Form: August 29, 2006

Nonaqueous reactions between titanium(IV) chloride and alcohols (benzyl alcohol or *n*-butanol) were used for the synthesis of anatase TiO_2 particles, while rutile TiO_2 particles were synthesized in aqueous media by acidic hydrolysis of titanium(IV) chloride. The X-ray diffraction measurements proved the exclusive presence of either the anatase or the rutile phase in prepared samples. The photoluminescence of both kinds of particles (anatase and rutile) with several well-resolved peaks extending in the visible spectral region was observed, and the quantum yield at room temperature was found to be 0.25%. Photon energy up-conversion from colloidal anatase and rutile TiO_2 particles was observed at low excitation intensities. The energy of up-converted photoluminescence spans the range of emission of normal photoluminescence. The explanation of photon energy up-conversion involves mid-gap energy levels originating from oxygen vacancies.

Introduction

One very important recent development in semiconductor nanoscience is the ability to control the size and shape of colloidal nanomaterials.[1,2] Size and shape control provides more flexibility and options for the design of new material to satisfy unique requirements. Nanosized titanium dioxide (TiO_2) particles have been the subject of a great deal of research because of their unique physicochemical properties and applications in the areas of pigments, gas sensors, catalysis, photocatalysts, photovoltaics, optics, inorganic membranes, and dielectric materials.[3−12] It is not surprising in view of the importance of TiO_2 nanoparticles that a wide variety of approaches for the synthesis of nanosized TiO_2 have been reported, and it remains a particularly active research field.

Literature data show that optical properties of TiO_2 significantly depend on the method of its synthesis and purification, the presence of dopants and defects in it, its surface state, and the way of its treatment. Although methods such as flame synthesis,[13,14] ultrasonic irradiation,[15,16] chemical vapor synthesis,[17] and hydrothermal methods[18−20] have been widely used, sol−gel processes have been shown to be especially versatile synthesis procedures.[21−27] Sol−gel reactions allow good control from the molecular precursors to the final product, which makes possible the low-temperature tailoring of materials to have high purity, high homogeneity, and desired size and morphology. Most of these sol−gel methods are based on the hydrolysis of an alkoxide or halide precursors and subsequent condensation to the inorganic framework. However, in most cases, sol−gel-derived precipitates at low temperatures are amorphous, and ultrasonic irradiation, subsequent hydrothermal processing, or calcination is necessary to induce crystallization. To overcome many of the specific problems for aqueous systems, nonhydrolytic sol−gel process have been developed. However, oxide formation requires temperatures in the range from 80 to 300 °C.[28] Here, we report a nonhydrolytic procedure to synthesize anatase TiO_2 particles in mild experimental conditions using reactions between $TiCl_4$ and benzyl alcohol or *n*-butanol. Also, we report aqueous synthesis of rutile TiO_2 under mild experimental conditions also using $TiCl_4$ as a precursor.

Considering photoluminescence (PL) spectroscopy as a highly sensitive tool to study the photophysics of the photogenerated species we have investigated electronic properties of both kinds of TiO_2 particles (anatase and rutile). We found out that synthesized anatase as well as rutile TiO_2 particles are emissive with well-resolved PL spectra extending in the visible spectral region due to the presence of oxygen vacancies.

Photon energy up-conversion (UC) in semiconductors (the observation of an emission at energies higher than the excitation energy) has attracted much attention recently. Such UC effects have been reported in bulk semiconductors,[29,30] heterostructures,[31−37] and self-assembled quantum dots.[38,39] For UC in bulk semiconductors and heterostructures, the proposed mechanism involves either a two-step photoexitation process[33−35,37] or an Auger recombination that ionizes carriers to the higher band gap region where they undergo radiative recombination.[31,32,36] Recently, photon energy UC has been observed in colloidal InP,[40] CdSe,[40] CdTe,[41] and core−shell CdSe/ZnS quantum dots[41,42] as well as Si nanocrystals.[43] In the case of colloidal quantum dots, the proposed mechanism is based on surface states and phonon processes.[40−42] Here, we report photon energy UC in colloidal TiO_2. The energy of the up-converted PL spans the range of energies displayed by the normal PL of the TiO_2. Much experimental evidence indicates that intraband surface states are involved in the UC-PL process.

Experimental Section

The anatase TiO_2 particles were synthesized by modifying the colloidal chemistry method already described in the literature.[44] In a typical preparation 2.5 mL of $TiCl_4$ (Fluka) was

† Part of the special issue "Arthur J. Nozik Festschrift".

* Author to whom correspondence should be addressed. Phone: +381-11-806-64-28. Fax: +381-11-244-73-82. E-mail: jovned@vin.bg.ac.yu.

‡ Vinča. Institute of Nuclear Sciences.

§ National Renewable Energy Laboratory.

10.1021/jp064454f CCC: $33.50
Published on Web 10/11/2006

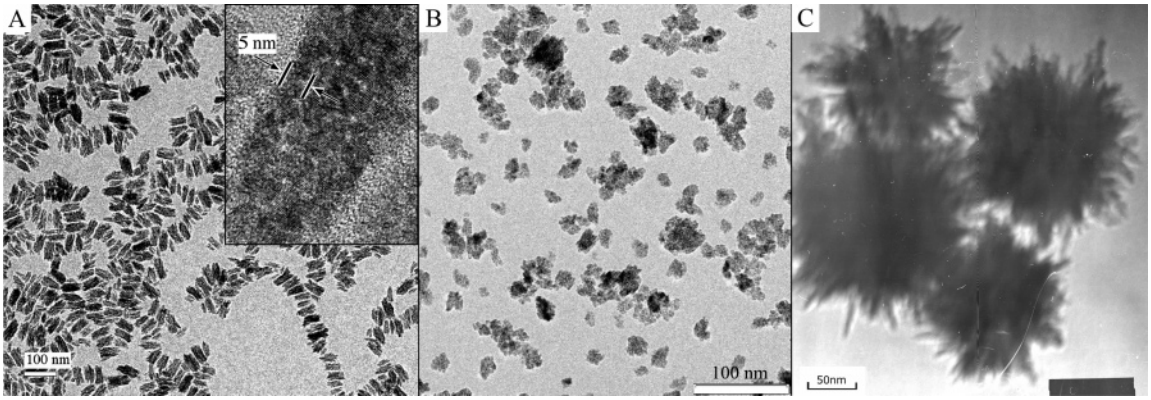

Figure 1. TEM images of TiO_2 samples: (A) anatase TiO_2 particles prepared in the reaction between $TiCl_4$ and benzyl alcohol (inset is HRTEM image), (B) anatase TiO_2 particles prepared in the reaction between $TiCl_4$ and *n*-butanol, and (C) rutile TiO_2 particles prepared by acidic hydrolysis of $TiCl_4$.

slowly added to 50 mL of anhydrous benzyl alcohol (Aldrich) or *n*-butanol (Fluka), under vigorous stirring at 0 °C. Caution should be taken as the reaction is rather violent. After 30 min the reaction vessel was sealed and under continuous stirring the sol was kept at 70 °C for 3 days. For optical measurements the resulting white dispersion was centrifuged at 5000 rpm, and the precipitate was thoroughly washed with ethanol and dispersed in tetrahydrofuran (THF) (J. T. Baker, HPLC grade). When necessary, THF was exchanged with solvents of different polarities, such as xylene, methanol, and water.

The rutile TiO_2 particles were synthesized modifying a "low-temperature dissolution−reprecipitation process" already described in the literature.[45] Briefly, 1.25 mL of $TiCl_4$ was slowly added to 50 mL of water, under vigorous stirring at 5 °C. The reaction vessel was kept at low temperature for 2 h, then it was sealed, and under continuous stirring the sol was kept at 45 °C for 2 days. The obtained dispersion was dialyzed against water to remove chloride ions.

For transmission electron microscopy (TEM) measurements, a droplet of oleylamine (Aldrich) was added to cleaned-up TiO_2 dispersed in organic solvent. All samples were extensively ultrasonicated for a few hours before deposition on a C-coated Cu grid. Microstructural characterization was performed on a Philips EM-400 transmission electron microscope operating at 100 kV, while high-resolution TEM (HRTEM) images where obtained on a Tecnai 20 Twin microscope.

The X-ray diffraction (XRD) analysis of TiO_2 powders, obtained after filtration through corresponding ultrafilters, was performed by using a Philips PW 1710 diffractometer.

Spectrophotometric measurements of colloidal TiO_2 were carried out on a Perkin-Elmer Lambda 5 UV−vis spectrophotometer, while PL spectra were recorded on a Perkin-Elmer LS-3b instrument. In addition, to obtain PL spectra with a true monochromatic excitation a diode-pumped solid-state laser Nd:YAG operating at 2.33 eV was used as an excitation source (the output power was up to 170 mW); the detection system was an Avantes S2000 spectrometer equipped with a 2048 element linear CCD array. Concentrations of the colloidal TiO_2 samples were in the range from 1.6×10^{-3} to 1.42×10^{-2} M. The PL quantum yield of the colloidal TiO_2 particles was determined by comparison of the wavelength-integrated emission intensity to that of quinine sulfate as a standard. For quantum yield determination excitation at 3.4 eV was used, while the concentrations of the colloidal TiO_2 nanorods and quinine sulfate were adjusted so that their absorbances at the excitation wavelength were the same ($A_{365\ nm} = 0.1$).

Results and Discussion

Figure 1 shows TEM pictures of TiO_2 samples. The anatase TiO_2 prepared in the reaction between $TiCl_4$ and benzyl alcohol is shown in Figure 1A. TiO_2 bundles 35 ± 10 nm in length by 10 ± 5 nm in diameter can be observed. At higher magnification (see inset in Figure 1A), it can be noticed that the bundles consist of TiO_2 nanorods 3−5 nm in diameter. The TiO_2 nanorods are fairly uniform, indicating that the described synthetic procedure provides good control of both diameter and length. Since the original synthetic procedure leads to the formation of spherical nanoparticles the formation of well-defined TiO_2 nanorods most likely can be explained by the prolonged aging at elevated temperature.[44] This is in agreement with literature data concerning hydrothermal synthesis of TiO_2 rods.[46] A TEM image of the anatase TiO_2 particles prepared in the reaction between $TiCl_4$ and *n*-butanol is shown in Figure 1B. The observed aggregates do not have well-defined shapes, and they are in the size range from 5 to 10 nm. Since this sample was prepared under the same experimental conditions as the first one, its different morphology can be attributed to the change of the alcohol. A TEM image of the rutile TiO_2 bundles prepared by acidic hydrolysis of $TiCl_4$ is shown in Figure 1C. Flowerlike agglomerates with diameters in the size range from 100 to 150 nm can be observed. Flowerlike agglomerates consist of TiO_2 nanorods 3−5 nm in diameter. A similar morphology was observed after prolonged aging at room temperature of titania particles prepared by acidic hydrolysis of titanium tetrabutoxide in reverse micelles.[47]

Typical XRD patterns of the TiO_2 particles are given in Figure 2. Samples prepared by a nonhydrolytic sol−gel process (reactions between $TiCl_4$ and benzyl alcohol or $TiCl_4$ and *n*-butanol) have the pure anatase phase without any indication of other crystalline byproducts. All diffraction peaks of the sample prepared by aqueous hydrolysis of $TiCl_4$ can be assigned to the rutile phase; once again, there is no indication of any crystalline byproducts. It can be noticed that all three samples (anatase TiO_2 prepared in two different ways and rutile TiO_2) are highly crystalline. However, the peaks are relatively broad due to the nanosize of the crystals. Through the use of Scherrer's equation to determine the average crystallite size by peak broadening analysis, anatase nanocrystals with grain sizes of 5.6 and 7 nm were obtained for samples prepared in the reactions between $TiCl_4$ and benzyl alcohol or *n*-butanol, respectively. In the case of rutile nanocrystals, peak broadening analysis revealed the presence of grains with sizes of 5 nm. It can be noticed that the grain sizes obtained from the XRD measure-

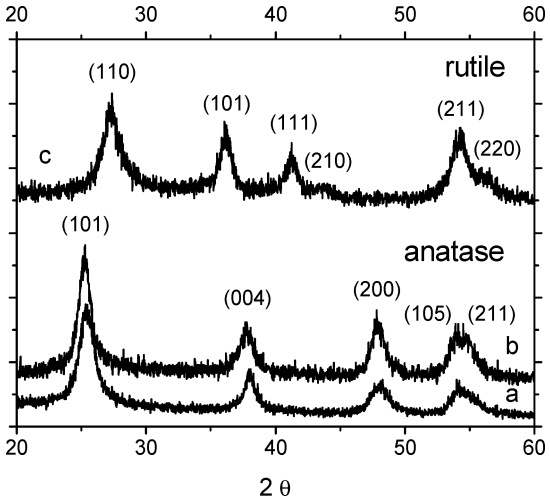

Figure 2. XRD pattern of TiO_2 samples: (a) anatase TiO_2 particles prepared in the reaction between $TiCl_4$ and benzyl alcohol, (b) anatase TiO_2 particles prepared in the reaction between $TiCl_4$ and *n*-butanol, and (c) rutile TiO_2 particles prepared by acidic hydrolysis of $TiCl_4$.

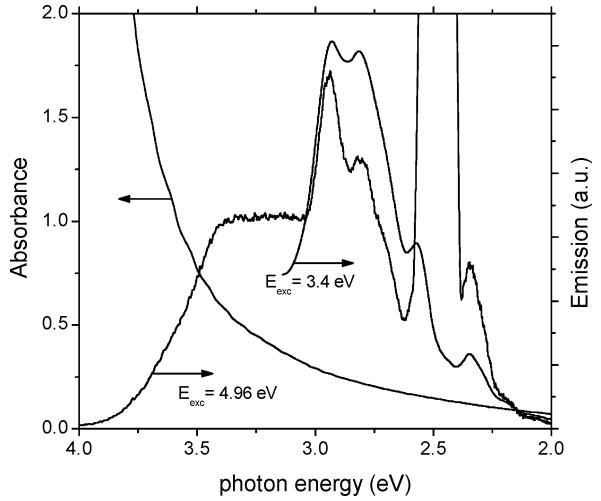

Figure 3. Absorption and PL spectra of dispersion consisting of the anatase TiO_2 particles in THF prepared in the reaction between $TiCl_4$ and benzyl alcohol.

ments correspond well to the diameters of anatase and rutile particles observed by TEM measurements.

Figure 3 shows the UV−vis absorption spectrum of anatase TiO_2 particles in THF prepared in the reaction between $TiCl_4$ and benzyl alcohol. A strong increase in absorption appears at about 3.18 eV indicating that absorption band edge of the TiO_2 particles corresponds well with the semiconductor band gap energy of crystalline bulk anatase (3.25 eV). The tail in the visible spectral region is a consequence of the light scattering due to the presence of TiO_2 bundles in solution. Also, the presence of oxygen vacancy states between the valence and the conduction bands in the TiO_2 band structure can contribute to the appearance of the visible light absorption (see further in the text).[48] PL spectra of anatase TiO_2 particles in THF with excitations at 4.96 and 3.40 eV are also presented in Figure 3. Broad emission in the spectral range from 3.8 to 3.1 eV was observed as well as the presence of well-resolved peaks/shoulders at 2.91, 2.80, 2.70, 2.56, and 2.34 eV. A change of solvent (xylene, methanol, water) did not decrease the intensity or change the shape and peak position of the PL spectra compared to the spectrum of the anatase TiO_2 particles in THF. The relative positions of the band energies are shown in Figure 4 with tentative assignments based on calculations by Daude et

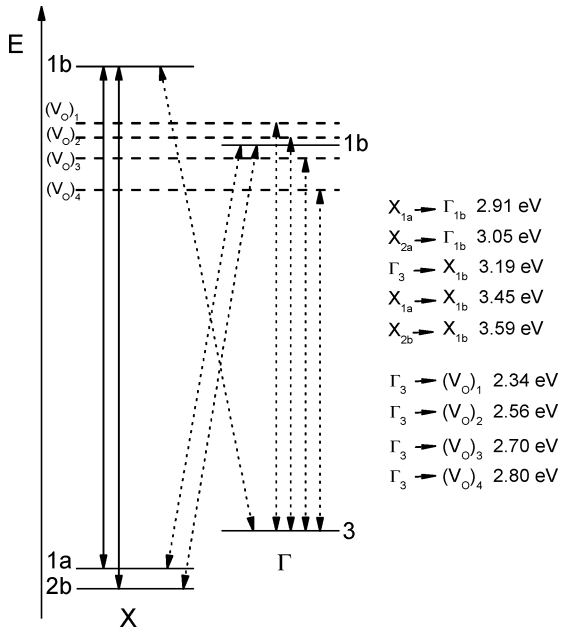

Figure 4. Energy level diagram illustrating the relative energy levels in the anatase TiO_2 as calculated in ref 49.

al.[49] A broad high-energy PL band spans the energy range that corresponds to direct transitions $X_{1b} \rightarrow X_{2b}$ (3.59 eV) and $X_{1b} \rightarrow X_{1a}$ (3.45 eV) as well as indirect transitions $X_{1b} \rightarrow \Gamma_3$ (3.19 eV) and $\Gamma_{1b} \rightarrow X_{2b}$ (3.05 eV). A well-defined PL peak corresponding to the lowest indirect transition $\Gamma_{1b} \rightarrow X_{1a}$ (2.91 eV) was also observed. In addition PL measurements revealed the presence of four shallow trap levels at energies of 2.80, 2.70, 2.56, and 2.34 eV. We assign high-energy peaks to band edge luminescence of the anatase TiO_2 particles, while we believe that lower-energy peaks/shoulders are induced by the presence of the oxygen vacancies. A similar PL spectrum was reported by Serpone et al.[50] for TiO_2 ultrafine particles prepared by controlled hydrolysis of titanium butoxide. These authors indicated the same positions of shallow trap levels after deconvolutive fitting of broad PL spectra obtained from colloidal TiO_2 particles with diameters of 2.1, 13.3, and 26.7 nm. However, the obtained PL spectrum is quite different compared to the PL spectrum reported by Niederberger et al.[44] These authors observed a single PL peak. These differences can be explained by a different degree of formed oxygen vacancies due to different experimental conditions (temperature, aging time) during synthesis.

It is important to point out that PL features of the anatase particles prepared in two different ways (reactions between $TiCl_4$ with butyl alcohol or *n*-butanol) are almost the same (Figure 5). For comparison the PL spectrum of rutile particles is also included in Figure 5. A difference between high-energy bands of rutile and anatase particles due to different band structures can be noticed. However, the positions of the shallow trap levels are the same, indicating the same origin, i.e., the presence of oxygen vacancies in rutile as well as anatase particles.

The PL quantum yield of the TiO_2 particles in solution was determined by comparison of the wavelength-integrated emission intensity to that of quinine sulfate as a standard. For all samples we found a quantum yield of approximately 0.25%. The obtained quantum yield is 4 times smaller compared to the result obtained by Niederberger et al.[44] Most likely this difference is a consequence of a modification of the original synthetic procedure. There are not many studies concerning the PL of TiO_2 particles. PL in TiO_2 particles was observed at

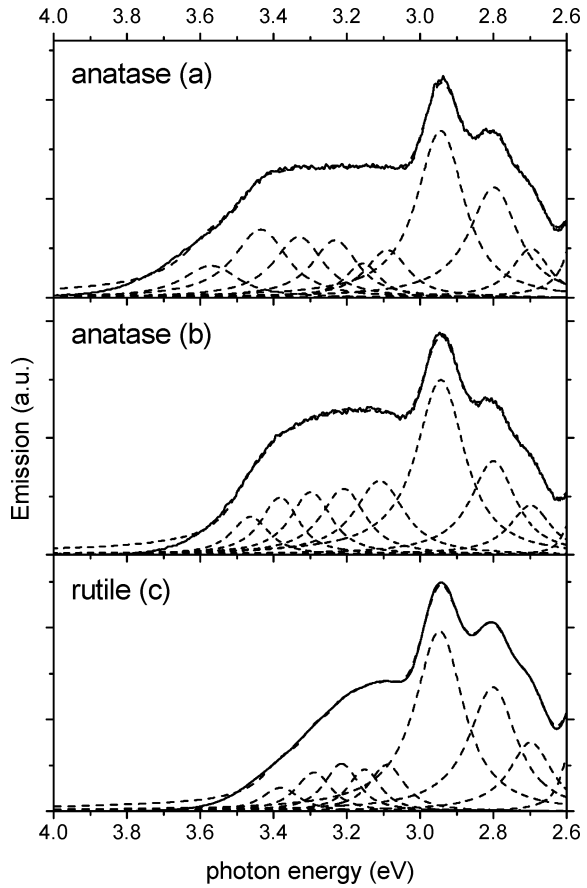

Figure 5. PL spectra of colloids consisting of (a) anatase TiO_2 particles prepared in the reaction between $TiCl_4$ and benzyl alcohol, (b) anatase TiO_2 particles prepared in the reaction between $TiCl_4$ and *n*-butanol, and (c) rutile TiO_2 particles prepared by acidic hydrolysis of $TiCl_4$.

temperatures of liquid nitrogen or lower,[51,52] while in most of the cases photoluminescent TiO_2 particles at room temperature were prepared either by using alcohol to hydrolyze $TiCl_4$ or in reactions where alkoxides were used as precursors.[44,53−56] These synthetic procedures lead to the formation of alkoxy (Ti−OR) groups instead of hydroxyl (Ti−OH) groups on the surfaces of TiO_2 particles. It seems that Ti−OR groups block surface traps, thus promoting radiative recombination.

The PL spectra of the rutile particles with excitation energies smaller than the band gap energy of TiO_2 obtained using a commercial fluorimeter are shown in Figure 6. UC spectra (excitation energies of 2.38, 2.21, and 2.07 eV) have the same positions of peaks/shoulders and similar intensities compared to the normal PL spectrum of the rutile. The UC spectra of the anatase particles also preserved all of the features of the normal PL spectra. These results are different than the published UC-PL results on InP quantum dots;[40] the UC-PL spectra of InP quantum dots do not have a peak. Most likely this difference can be explained by the small degree of surface traps on InP quantum dots due to postsynthetic treatment with HF. It was found out for anatase and rutile particles that the lowest excitation photon energy for which the UC-PL still can be detected is 1.89 eV. To exclude any ambiguity additional experiments were performed using a diode-pumped solid-state laser Nd:YAG operating at 2.33 eV as a monochromatic excitation source instead of a commercial fluorimeter. Typical UC spectra of the anatase particles obtained using laser excitation are shown in Figure 7. The positions of the peaks remained the same, but they became much sharper with two very narrow lines at 2.92 and 2.84 eV. Similar UC spectra were

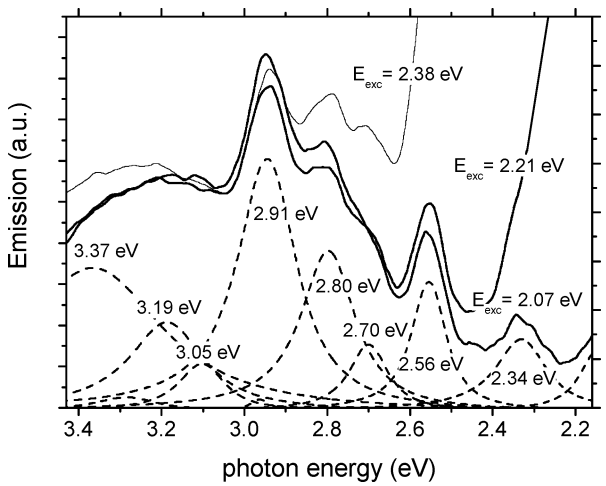

Figure 6. UC-PL spectra of the rutile TiO_2 particles measured with a commercial fluorimeter.

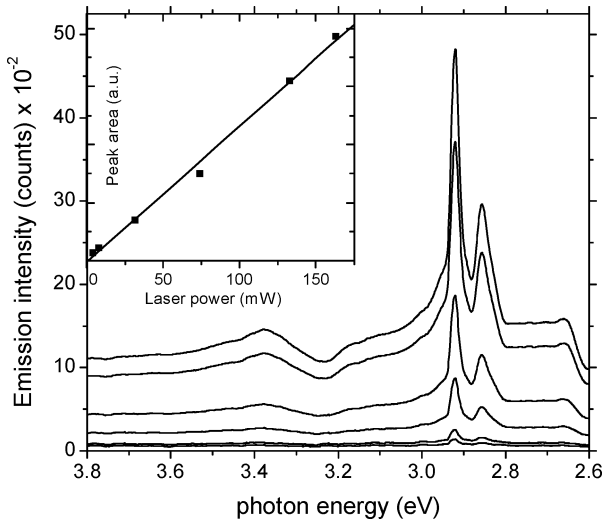

Figure 7. Typical UC-PL spectra of the anatase TiO_2 particles prepared in the reaction between $TiCl_4$ and benzyl alcohol and measured using laser excitation. The dependence between UC-PL intensity and excitation intensity is given in inset.

reported by Wang et al.[57] These authors reported an intense UC line at 2.88 eV with TiO_2 nanoparticle films, using for excitation a He−Cd laser operating at 2.81 eV. (The output power of the laser was 70 mW.) Dependence of the UC-PL intensity in anatase particles on the output excitation power at room temperature is shown in the inset of Figure 7. We found that the UC-PL is a linear function of the excitation intensity; the same dependence was found for rutile particles. Linear dependence between UC-PL and excitation intensity was also found by Rusakov et al.[42] in core−shell CdSe/ZnS quantum dots.

On the basis of these results, we can highlight several important features in the UC-PL spectra. First, the relative intensity of the UC-PL is similar to the intensity of the normal PL with the same positions of the peaks/shoulders. Second, the UC-PL is not visible for excitation energies lower than 1.89 eV. Third, the UC-PL spectra were obtained at low light intensity (a Xe lamp in the spectrofluorophotometer was used as the excitation source as well as a Nd:YAG laser operating at 2.33 eV with an output power up to 170 mW). Also, the linear dependence between the UC-PL intensity and excitation intensity was observed. The fourth feature in the UC-PL is the critical role of mid-gap trap states originating from oxygen vacancies.

The commonly discussed mechanisms leading to photon energy UC are Auger recombination, nonlinear multiphoton processes, and thermal activation by the absorption of phonons. The Auger recombination (cubic dependence on excitation intensity) or nonlinear two-photon absorption (quadratic dependence on excitation intensity) cannot be the cause of the observed photon energy UC since linear dependence was observed. In addition, the lamp excitation source is too weak to induce multiphoton processes. The observed UC-PL most likely originates from cascade excitation involving mid-gap trap states, i.e., from the valence band to intraband trap state located near the conduction band and subsequent thermally activated detrapping from the intraband trap state to the conduction band, followed by recombination from the conduction band or mid-gap energy levels to the valence band. The observed UC-PL in colloidal anatase and rutile particles as well as the proposed mechanism are in a good agreement with previously reported data concerning InP,[40] CdSe,[40] CdTe,[41] and core−shell CdSe/ZnS quantum dots.[41,42]

In conclusion, we report synthetic procedures for preparation of TiO_2 particles in mild experimental conditions with exclusive presence of either the anatase or the rutile phase. PL and UC-PL of both kinds of particles extending to the visible spectral region were observed, and a mechanism that involves mid-gap energy levels originating from oxygen vacancies is proposed. Since the UC-PL mechanism is still open to debate, studies concerning the excited-state lifetimes will be the subject of our future work.

Acknowledgment. The authors are grateful for the use of facilities in the National Renewable Energy Labororatory Biomass Surface Characterization Laboratory. Financial support for this study was granted by the Ministry of Science and Environmental Protection of the Republic of Serbia (Project No. 142066).

References and Notes

(1) Jun, Y.; Casula, M. F.; Sim, J.-H.; Kim, S. Y.; Cheon, J.; Alivisatos, A. P. *J. Am. Chem. Soc.* **2003**, *125*, 15981−15985.
(2) Cozzoli, P. D.; Kornowski, A.; Weller, H. *J. Am. Chem. Soc.* **2003**, *125*, 14539−14548.
(3) Anpo, M.; Shima, T.; Kodama, S.; Kubokawa, Y. *J. Phys. Chem.* **1987**, *91*, 4305−4310.
(4) O'Regan, B.; Gratzel, M. *Nature* **1991**, *353*, 737−740.
(5) Choi, W.; Termin, A.; Hoffmann, M. R. *J. Phys. Chem.* **1994**, *98*, 13669−13679.
(6) Bach, U.; Lupo, D.; Comte, P.; Moser, J. E.; Weissortel, F.; Salbeck, J.; Spreitzer, H.; Gratzel, M. *Nature* **1998**, *395*, 583−585.
(7) Will, G.; Rao, J.; Fitzmaurice, D. *J. Mater. Chem.* **1999**, *9*, 2297−2299.
(8) Park, N.-G.; van de Lagemaat, J.; Frank, A. J. *J. Phys. Chem. B* **2000**, *104*, 8989−8994.
(9) Morris, D.; Egdell, R. G. *J. Mater. Chem.* **2001**, *11*, 3207−3210.
(10) Stark, W. J.; Wegner, K.; Pratsinis, S. E.; Baiker, A. *J. Catal.* **2001**, *197*, 182−191.
(11) Feldmann, C. *Adv. Mater.* **2001**, *13*, 1301−1303.
(12) Frindell, K. L.; Bartl, M. H.; Popitsch, A.; Stucky, G. D. *Angew. Chem., Int. Ed.* **2002**, *41*, 959−962.
(13) Morrison, P. W.; Raghavan, R.; Timpone, A. J.; Artelt, C. P.; Pratsinis, S. E. *Chem. Mater.* **1997**, *9*, 2702−2708.
(14) Yang, G.; Zhuang, H.; Biswas, P. *Nanostruct. Mater.* **1996**, *7*, 675−689.
(15) Yu, J. C.; Yu, J.; Ho, W.; Zhang, L. *Chem. Commun.* **2001**, 1942−1943.
(16) Huang, W. P.; Tang, X. H.; Wang, Y. Q.; Koltypin, Y.; Gedanken, A. *Chem. Commun.* **2000**, 1415−1416.
(17) Seifried, S.; Winterer, M.; Hahn, H. *Chem. Vap. Deposition* **2000**, *6*, 239−244.
(18) Cheng, H., Ma, J.; Zhao, Z.; Qi, L. *Chem. Mater.* **1995**, *7*, 663−671.
(19) Wang, C. C.; Ying, J. Y. *Chem. Mater.* **1999**, *11*, 3113−3120.
(20) Aruna, S. T.; Tirosh, S.; Zaban, A. *J. Mater. Chem.* **2000**, *10*, 2388−2391.
(21) Zhang, Z. B.; Wang, C. C.; Zakaria, R.; Ying, J. Y. *J. Phys. Chem. B* **1998**, *102*, 10871−10878.
(22) Scolan, E.; Sanchez, C. *Chem. Mater.* **1998**, *10*, 3217−3223.
(23) Schneider, M.; Baiker, A. *J. Mater. Chem.* **1992**, *2*, 587−591.
(24) Chen, J. Y.; Gao, L.; Huang, J. H.; Yan, D. S. *J. Mater. Sci.* **1996**, *31*, 3497−3500.
(25) Ivanda, M.; Music, S.; Popovic, S.; Gotic, M. *J. Mol. Struct.* **1999**, *481*, 645−649.
(26) Zhang, H.; Finnegan, M.; Banfield, J. F. *Nano Lett.* **2001**, *1*, 81−85.
(27) Burnside, S. D.; Shklover, V.; Barbe, C.; Comte, P.; Arendse, F.; Brooks, K.; Gratzel, M. *Chem. Mater.* **1998**, *10*, 2419−2425.
(28) Trentler, T. J.; Denler, T. E.; Bertone, J. F.; Agrawal, A.; Colvin, V. L. *J. Am. Chem. Soc.* **1999**, *121*, 1613−1614.
(29) Johnson, E. J.; Kafalas, J.; Davies, R. W.; Dyes, W. A. *Appl. Phys. Lett.* **1982**, *40*, 993−995.
(30) Ivanov, V. Yu.; Semenov, Yu. G.; Surma, M.; Godlewski, M. *Phys. Rev. B* **1996**, *54*, 4696−4701.
(31) Seidel, W.; Titkov, A.; André, J. P.; Voisin, P.; Voos, M. *Phys. Rev. Lett.* **1994**, *73*, 2356−2359.
(32) Driessen, F. A. J. M.; Cheong, H. M.; Mascarenhas, A.; Deb, S. K.; Hageman, P. R.; Bauhuis, G. J.; Giling, L. J. *Phys. Rev. B* **1996**, *54*, R5263−R5266.
(33) Zeman, J.; Martinez, G.; Yu. P. Y.; Uchida, K. *Phys Rev B* **1997**, *55*, R13428−R13431.
(34) Cho, Y.-H.; Kim, D. S.; Choe, B.-D.; Lim, H.; Lee, J. I.; Kim, D. *Phys. Rev. B* **1997**, *56*, R4375−R4378.
(35) Schrottke, L.; Grahn, H. T.; Fujiwara, K. *Phys. Rev. B* **1997**, *56*, R15553−R15556.
(36) Cheong, H. M.; Fluegel, B.; Hanna, M. C.; Mascarenhas, A. *Phys. Rev. B* **1998**, *58*, R4254−R4257.
(37) Heimbrodt, W.; Happ, M.; Henneberger, F. *Phys. Rev. B* **1999**, *60*, R16326−R16329.
(38) Paskov, P. P.; Holtz, P. O.; Monemar, B.; Garcia, J. M.; Schoenfeld, W. V.; Petroff, P. M. *Appl. Phys. Lett.* **2000**, *77*, 812−814.
(39) Kammerer, C.; Cassabois, G.; Voisin, C.; Delalande, C.; Roussignol, Ph.; Gerrard, J. M. *Phys. Rev. Lett.* **2001**, *87*, 2074011−2074014.
(40) Poles, E.; Selmarten, D. C.; Mićić, O. I.; Nozik, A. J. *Appl. Phys. Lett.* **1999**, *75*, 971−973.
(41) Rakovich Yu. P.; Filonovich, S. A.; Gomes, M. J. M.; Donegan, J. F.; Talapin, D. V.; Rogach, A. L.; Eychmuller, A. *Phys. Status Solidi B* **2002**, *229*, 449−452.
(42) Rusakov, K. I.; Gladyshchuk, A. A.; Rakovich, Yu. P.; Donegan, J. F.; Filonovich, S. A.; Gomes, M. J. M.; Talapin, D. V.; Rogach, A. L.; Eychmüller, A. *Opt. Spectrosc.* **2003**, *94*, 859−863.
(43) Diener, J.; Kovalev, D.; Heckler, H.; Polisski, G.; Künzner, N.; Koch, F.; Efros, Al. L.; Rosen, M. *Opt. Mater.* **2001**, *17*, 135−139.
(44) Niederberger, M.; Bartl, M. H.; Stucky, G. D. *Chem. Mater.* **2002**, *14*, 4364−4370.
(45) Yin, S.; Hasegawa, H.; Maeda, D.; Ishitsuka, M.; Sato, T. *J. Photochem. Photobiol., A* **2004**, *163*, 1−8.
(46) Miao, L.; Tanemura, S.; Toh, S.; Kaneko, K.; Tanemura, M. *Appl. Surf. Sci.* **2004**, *238*, 175−179.
(47) Zhang, D.; Qi, L.; Ma, J.; Cheng, H. *J. Mater. Chem.* **2002**, *12*, 3677−3680.
(48) Nakamura, J.; Negishi, N.; Kutsuna, S.; Ihara, T.; Sugihara, S.; Takeuchi, K. *J. Mol. Catal.* **2000**, *161*, 205−212.
(49) Daude, N.; Gout, C.; Jouanin, C. *Phys. Rev. B* **1977**, *15*, 3229−3235.
(50) Serpone, N.; Lawless, D.; Khairutdinov, R. *J. Phys. Chem.* **1995**, *99*, 16646−16654.
(51) Anpo, M.; Aikawa, N.; Kubokawa, Y.; Che, M.; Louis, C.; Giamello, E. *J. Phys. Chem.* **1985**, *89*, 5017−5021.
(52) Anpo, M.; Tomonari, M.; Fox, M. A. *J. Phys. Chem.* **1989**, *93*, 7300−7302.
(53) Zhu Y.; Ding, C.; Ma G.; Du Z. *J. Solid State Chem.* **1998**, *139*, 124−127.
(54) Zhu Y. C.; Ding, C. X. *J. Solid State Chem.* **1999**, *145*, 711−715.
(55) Zhang, W. F.; Zhang, M. S.; Yin, Z.; Chen, Q. *Appl. Phys. B* **2000**, *70*, 261−265.
(56) Jung, K. Y.; Park, S. B.; Anpo, M. *J. Photochem. Photobiol., A* **2005**, *170*, 247−252.
(57) Wang, C.; Li, Q.; Xiong, G. *J. Mater. Sci.* **2004**, *39*, 5581−5582.